CENTER FOR INFRASTRUCTURE ENGINEERING STUDIES

GEOPHYSICAL ASSESSMENT OF KARST ACTIVITY

by

Neil L. Anderson

A University Transportation Center Program
at Missouri University of Science & Technology

Disclaimer

The contents of this report reflect the views of the author(s), who are responsible for the facts and the accuracy of information presented herein. This document is disseminated under the sponsorship of the Department of Transportation, University Transportation Centers Program and the Center for Infrastructure Engineering Studies UTC program at the University of Missouri - Rolla, in the interest of information exchange. The U.S. Government and Center for Infrastructure Engineering Studies assumes no liability for the contents or use thereof.

Technical Report Documentation Page

1. Report No.	2. Government Accession No.	3. Recipient's Catalog No.
UTC R189		

4. Title and Subtitle	5. Report Date
GEOPHYSICAL ASSESSMENT OF KARST ACTIVITY	February 2008
	6. Performing Organization Code

7. Author/s	8. Performing Organization Report No.
Neil L. Anderson	00015328

9. Performing Organization Name and Address	10. Work Unit No. (TRAIS)
Center for Infrastructure Engineering Studies/UTC program Missouri University of Science & Technology 223 Engineering Research Lab Rolla, MO 65409	11. Contract or Grant No. DTRS98-G-0021

12. Sponsoring Organization Name and Address	13. Type of Report and Period Covered
U.S. Department of Transportation Research and Special Programs Administration 400 7th Street, SW Washington, DC 20590-0001	Final
	14. Sponsoring Agency Code

15. Supplementary Notes

16. Abstract

MST proposes to acquire electrical resistivity data within a pipeline/roadway ROW. These geophysical data will be processed, analyzed and interpreted with the objective of locating and mapping any subsurface voids that might compromise the integrity of the pipeline/roadway. The main project deliverable will be a map showing the location and estimated depth of any voids.

17. Key Words	18. Distribution Statement
non-destructive imaging, non-invasive imaging, technology transfer, education	No restrictions. This document is available to the public through the National Technical Information Service, Springfield, Virginia 22161.

19. Security Classification (of this report)	20. Security Classification (of this page)	21. No. Of Pages	22. Price
unclassified	unclassified	12	

Form DOT F 1700.7 (8-72)

GEOPHYSICAL ASSESSMENT OF KARST ACTIVITY

Neil L. Anderson (nanders@umr.edu)

Department of Geological Engineering and Sciences
127 McNutt Hall, University of Missouri-Rolla, Rolla, MO 65409

EXECUTIVE SUMMARY

A geophysical data set consisting of ten electrical resistivity profiles and two MASW (acronym for **m**ultichannel **a**nalyses of **s**urface **w**aves) profiles were acquired along traverses in immediate proximity to two active sinkholes at the study site. Analysis of the acquired geophysical data supports the conclusion that that none of the ten traverses (with the possible exception of traverse 5) overlies air-filled subsurface voids of any significant size. The data also support the conclusion that sinkholes #1 and #3 developed along or adjacent to N/S-trending solution-widened joints/fractures which do not appear to extend beneath the traverses closest to the buried utility of interest.

INTRODUCTION

Geophysical data were acquired at the study site in order to image and characterize the shallow subsurface in proximity to visually-identified sinkholes #1 and #3 (Figure 1). Electrical resistivity profiles were acquired along ten traverses (two grids of five traverses each); MASW profiles were acquired along two of the ten traverses (Figure #1).

The primary objective was to determine if air-filled cavities of karstic origin were present beneath any of the ten traverses. Secondary objectives were: 1) to provide the consulting geologist with 2-D images of the subsurface so that conclusions could be drawn regarding the potential for further karstic activity in the study area, and 2) to determine the engineering properties (shear wave velocity) of the soil and rock.

The electrical resistivity tool was employed because it is uniquely designed to image air-filled voids, and to differentiate clay, intensely weathered rock, fractured rock and intact rock. The MASW tool was employed because it is uniquely designed to measure the shear wave velocity of the soil.

ELECTRICAL RESISTIVITY DATA

Two-dimensional electrical resistivity profiling is commonly used to image the shallow subsurface (depths <100 ft) in karst terrain because air-filled voids, clay, intensely weathered rock, fractured rock and intact rock can normally be differentiated and mapped on 2-D resistivity profiles (Figure 2) (Anderson et al., 2006; FHWA, 2003). Clays in the study area are normally characterized by low resistivities (variable, depending on moisture content, purity, and unit shape/size, but usually less than 100 ohm-m). Intensely weathered rock (intermixed with clay) is typically characterized by resistivities of between 100 and 400 ohm-m. Fractured to intact limestone is generally characterized by higher resistivites (typically more than 400 ohm-m, but variable depending on layer thickness, moisture content and impurities). Air-filled voids are normally characterized by very high resistivities (typically >20000 ohm-m, but variable depending on the conductivity of the encompassing strata and depth/size/shape of void).

The resistivity tool frequently provides a superior combination of spatial resolution and depth of investigation in karst terrain than any other non-invasive geophysical imaging technique. The resolution provided by the resistivity tool is a function of the electrode spacing, and other factors including subsurface heterogeneity and conductivity contrasts. During processing, the subsurface beneath the traverse is subdivided into rectangular pixels with lateral dimensions equal to the electrode spacing and vertical dimensions that are typically 25% (at shallowest depths) to 100% (at greatest depths) of the electrode spacing. Pixel size is one estimate of maximum spatial resolution. Additionally, the processing software assumes the subsurface is uniform in directions perpendicular to the traverse; hence some lateral and vertical smoothing (mixing) will occur in heterogeneous strata. The depth of investigation is a function of the length of the 2-D array employed. Maximum depths of investigation are typically 20 to 25% of the array length, varying primarily as a function of subsurface conductivities.

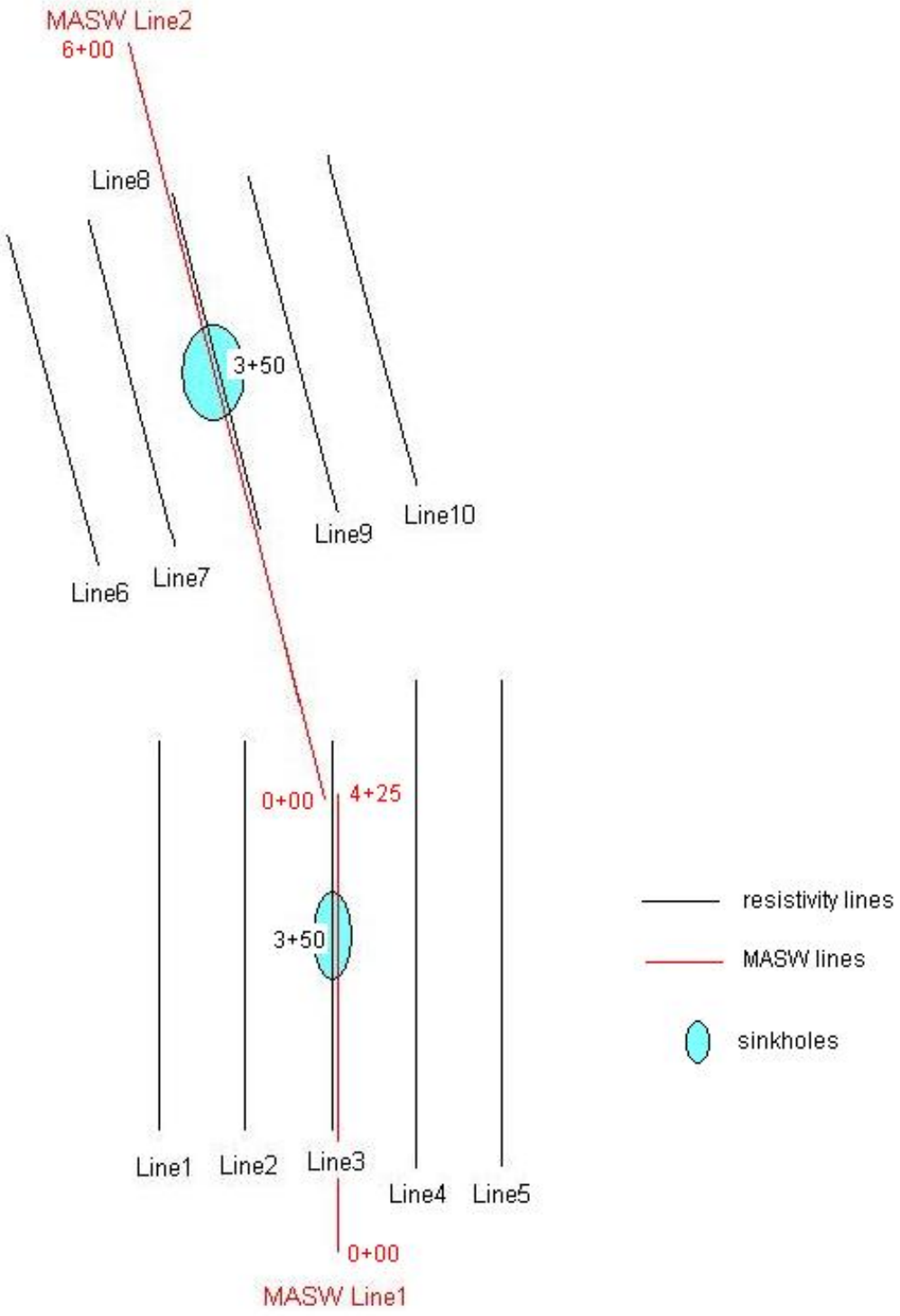

Figure #1: Base map showing relative locations and orientations of sinkholes #1 and #3, electrical resistivity profiles 1-10, and MASW profiles 1 and 2.

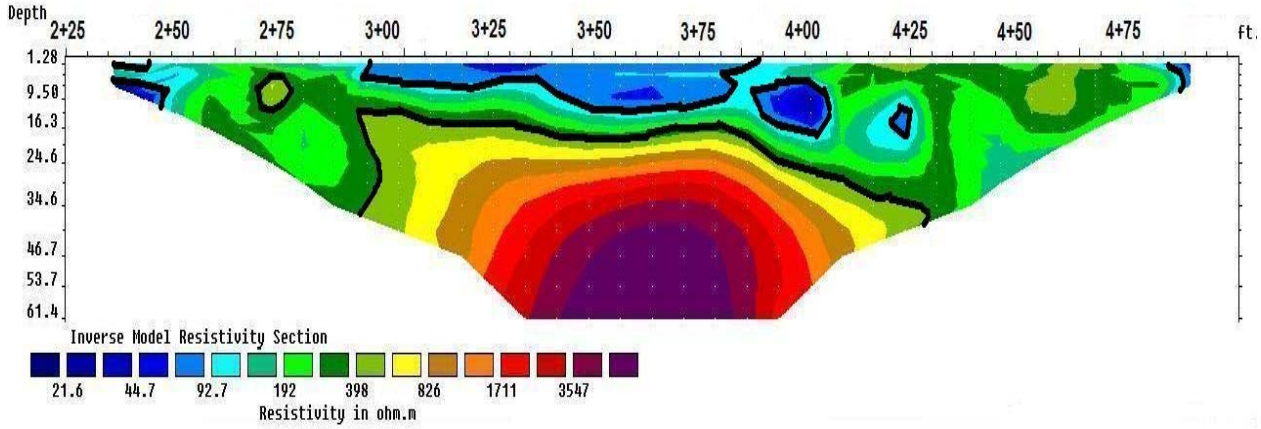

Figure 2: Example resistivity profile. Clays are normally characterized by low resistivities (variable, depending on moisture content, purity, and unit shape/size, but usually less than 100 ohm-m). Intensely weathered rock (intermixed with clay) is typically characterized by resistivities of between 100 and 400 ohm-m. Fractured to intact limestone is generally characterized by higher resistivites (typically more than 400 ohm-m, but variable depending on layer thickness, moisture content and impurities). Air-filled voids are normally characterized by very high resistivities (typically >20000 ohm-m, but variable depending on the conductivity of the encompassing strata and depth/size/shape of void).

MASW DATA

Two-dimensional MASW profiling is commonly used to determine the shear wave velocity of soil and rock in the shallow subsurface (depths <100 ft), mostly for engineering classification purposes (Figure 3). However, the MASW tool can also be used to differentiate soils and rock on the basis of their acoustic properties. Soils are normally characterized by low shear wave velocities (typically less than 1000 m/s, depending mostly on density and lithology), whereas fractured to intact limestone is characterized by higher shear wave velocities (typically more than 2000 m/s). Intensely weathered rock and rock with intermixed/interlayered clays are typically characterized by shear wave velocities of between 1000 and 2000 m/s. Air-filled voids are normally characterized by shear wave velocities that are non-zero, but anomalously low compared with those of the host strata. The non-zero "apparent" shear wave velocity of air-filled voids is attributable to lateral and vertical smoothing and the nature of the inversion software.

In karst terrain, the resolution of the MASW tool is normally significantly less than that provided by the electrical resistivity tool. The lower resolution of the MASW tool is attributable to the fact that shear wave velocities are measured (by necessity) using 25 ft long geophone arrays. The shear wave velocity at any depth at any station along an MASW profile represents the "average" velocity at that depth over a lateral distance of up to 25 ft. If subsurface lithologies vary significantly over that 25 ft window, significant lateral averaging will occur.

SINKHOLE #1

Resistivity profile 3 and MASW profile 1 tie sinkhole #1 near station 3+50 (Figure 1). The three boreholes (B4, B5 and B6) sited near sinkhole #1 also tie the geophysical traverses. Borehole B4 ties resistivity profile 3 and MASW profile 1 near station 3+90; borehole B5 ties resistivity profile #4 near station 3+50; borehole B6 ties resistivity profile 3 and MASW profile 1 near station 3+10.

Noninterpreted versions of resistivity profiles 1-5 are displayed in Figure 4. Interpreted versions of resistivity profiles 1-5 are displayed as Figures 5-9, respectively. MASW profile 1 is displayed as Figure 10. In an effort to validate the interpretations of the electrical resistivity and MASW data, we focus initially on the correlations between boreholes B4, B5 and B6 and the interpreted versions of resistivity profiles 3 and 4, and MASW profile 1 (Figures 7, 8 and 10).

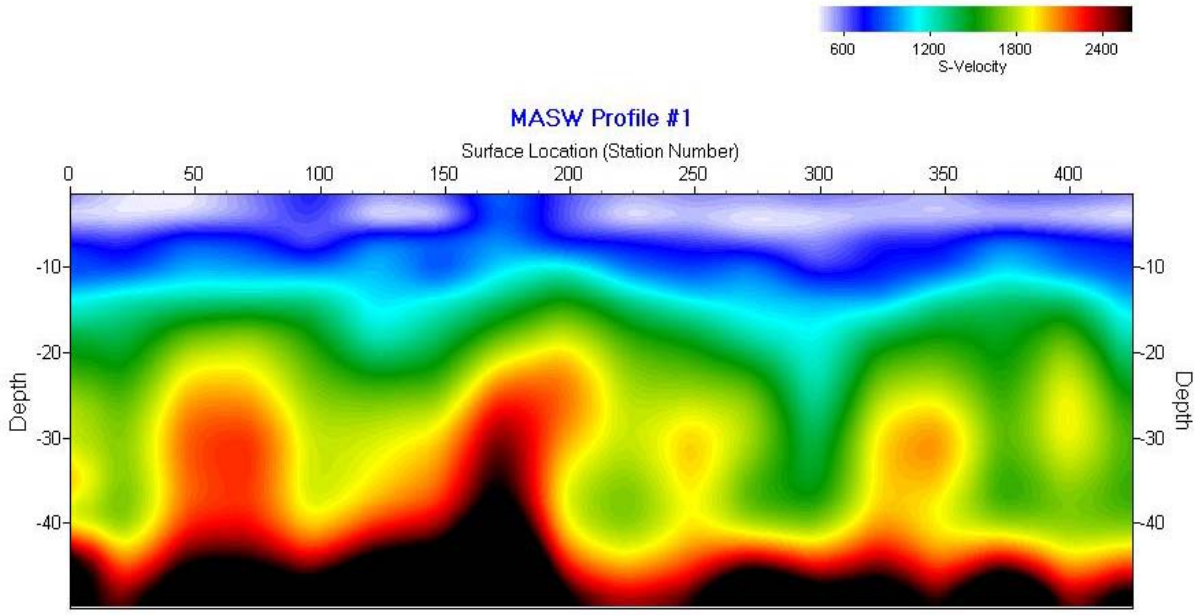

Figure 3: Example MASW profile. Soils are normally characterized by low shear wave velocities (typically less than 1000 m/s, depending mostly on density and lithology), whereas fractured to intact limestone is characterized by higher shear wave velocities (typically more than 2000 m/s). Intensely weathered rock and rock with intermixed/interlayered clays are typically characterized by shear wave velocities of between 1000 and 2000 m/s. Air-filled voids are normally characterized by shear wave velocities that are non-zero, but anomalously low compared with those of the host strata. The non-zero "apparent" shear wave velocity of air-filled voids is attributable to lateral and vertical smoothing and the nature of the inversion software.

Borehole B4, which ties resistivity profile 3 and MASW profile 1 near station 3+90, encountered 22 ft of red clay (medium to very stiff, dry to moist) with weathered limestone and chert, before terminating in grey, laminated, silicious limestone. Bedrock (top of intact limestone) on interpreted electrical resistivity profile 3 at station 3+90 is at a depth of 23 ft. The overlying 23 ft of strata on the resistivity profile would normally be interpreted as clay and/or intensely weathered rock intermixed with clay. The top of bedrock at station 3+90 is not so clearly imaged on MASW profile 1. However shear wave velocities on the order of 2000 ft/s (which typically constitutes top of intact rock) are first imaged at a depth of about 22 ft. In summary, the correlation between borehole B4 and the geophysical data is excellent.

Borehole B5, which ties resistivity profile 4 near station 3+50, encountered approximately 19 ft of moist, soft to very stiff clay w/wo limestone and chert, and 6 ft of moist, hard, red clay with weathered limestone and chert before terminating in hard, grey, fractured, laminated limestone (at a depth of 25 ft). Bedrock (top of intact limestone) on interpreted electrical resistivity profile 4 at station 3+50 is at a depth of about 20 ft. This 5 ft difference between the 25 ft (borehole) and 20 ft (resistivity) depths-to-bedrock could be attributable to the presence of 6 ft of hard clay immediately above borehole bedrock (which could have resistivities comparable to weathered bedrock), the fact that the borehole and the resistivity profiles do not tie exactly, and/or to the observation that depth to bedrock varies rapidly in proximity to station 3+50 (which could result in significant smoothing). We also note that bedrock beneath station 3+50 is characterized by a vertically-extensive zone of relatively low resistivities, suggesting that it is fractured. In our opinion, we are probably imaging the lateral extension of the solution-widened fracture that is the source of sinkhole #1. In summary, the correlation between borehole B4 and the geophysical data is good.

Borehole B6, which ties resistivity profile 3 and MASW profile 1 near station 3+10, encountered 28 ft of predominantly wet red clay (soft to medium stiff, dry to moist) and about 4 ft of moist, stiff to very stiff red clay with weathered limestone, before terminating in hard grey chert with clay lenses at a depth of 32 ft. Bedrock (top of intact rock) on interpreted electrical resistivity profile 3 at station 3+10 is at a depth of about 36 ft. The overlying 23 ft of strata on the resistivity profile would normally be interpreted as predominantly clay. The top of bedrock at station 3+10 is not so clearly imaged on MASW profile 1. However shear wave velocities on the order of 2000 ft/s (which typically constitutes top of intact rock) are first imaged at a depth of about 31 ft. In summary, the correlation between borehole B4 and the geophysical data is excellent.

The correlations between the borehole data and the geophysical data are good to excellent, and validate the interpretations presented in Figures 5-9. From our perspective, the two most significant conclusions that can be drawn from these interpretations are as follows:

Significant Interpretation 1: Sinkhole #1 appears to have developed near the northern edge of a prominent N/S-trending solution-widened fracture/joint that is imaged only on resistivity profiles 4 and 5. This solution-widened fracture/joint is centered at station 3+50 on resistivity profile 4, but widens considerably on profile 5. It is not observed on profile 3 which is located immediately to the north (within a couple of ft) of sinkhole #1.

Significant Interpretation 2: There is no geophysical evidence to suggest that the solution-widened fracture associated (apparently) with sinkhole #1 extends beneath traverses 1 0r 2 (which are closest to the buried utility of interest).

Significant Interpretation 3: There is no geophysical evidence to suggest that traverses 1, 2, 3 or 4 are underlain by substantive voids. However, we note that resistivity traverse 5 overlies four shallow anomalies with apparent resistivities in excess of 20000 ohm-m (Figure 9). In our opinion, these anomalies are most probably attributable to the presence of lenses of low-porosity intact cap rock. However, it is possible that the anomalies could be generated by air-filled voids within rock.

SINKHOLE #3

Resistivity profile 8 and MASW profile 2 tie sinkhole #1 near station 3+50 (Figure 1). The three boreholes (B1, B2 and B3) sited near sinkhole #3 also tie the geophysical traverses. Borehole B1 ties resistivity profile 7 near station 3+00; borehole B2 ties resistivity profile #10 near station 3+10; borehole B3 ties resistivity profile 10 and MASW profile 1 near station 3+60.

Noninterpreted versions of resistivity profiles 6-10 are displayed in Figure 11. Interpreted versions of resistivity profiles 6-10 are displayed as Figures 12-16, respectively. MASW profile 2 is displayed as Figure 17. In an effort to validate the interpretations of the electrical resistivity and MASW data, we focus initially on the correlations between boreholes B1, B2 and B3 and the interpreted versions of resistivity profiles 7 and 10 (Figures 13 and 16).

Borehole B1, which ties resistivity profile 7 near station 3+00, encountered about 13 ft of moist, slightly silty-sandy red clay (medium stiff to stiff) and approximately 7 ft of moist red clay w/wo weathered limestone before terminating in 4 ft of grey, laminated, silicious limestone with calcite-filled voids and kaolinite clay. Resistivity profile 8 at station 3+00 is reasonably consistent with these borehole data (Figure 13). More specifically, resistivity profile at station 3+00 consists of ~24 ft of low-intermediate resistivity material which probably corresponds to the shallow clay encountered in borehole B3. Bedrock (top of intact limestone) on interpreted electrical resistivity profile 7 at station 3+00 is at an estimated depth of 24 ft. In summary, the correlation between borehole B1 and the geophysical data is reasonably good.

Borehole B2, which ties resistivity profile 10 near station 3+10, encountered approximately 20 ft of moist, stiff to very stiff red clay with weathered limestone before terminating in hard, grey, silicious limestone. Bedrock (top of intact limestone) on interpreted electrical resistivity profile 10 at station 3+10 is at a depth of 20 ft (Figure 16). The correlation between borehole B4 and the geophysical data is excellent.

Borehole B3, which ties resistivity profile 10 near station 3+60, encountered 15 ft of moist, soft to very stiff red clay with weathered limestone before terminating in hard, grey, silicious limestone. Bedrock (top of intact limestone) on interpreted electrical resistivity profile 10 at station 3+10 is at a depth of 20 ft (Figure 16). The correlation between borehole B4 and the geophysical data is reasonably good. In summary, the correlation between borehole B4 and the geophysical data is excellent. [We note that borehole B3 appears to have been placed immediately adjacent to a solution-widened fracture/joint (centered at station 3+75 on profile 10; Figure 16) that appears to extend beneath traverses 8 and 9, and could be the cause of sinkhole #3.]

The correlations between the borehole data and the geophysical data are good to excellent, and validate the interpretations presented in Figures 12-16. From our perspective, the two most significant conclusions that can be drawn from these interpretations are as follows:

Significant Interpretation 4: Sinkhole #3 appears to have developed immediately to the west of a prominent N/S-trending solution-widened fracture/joint that is imaged on resistivity profiles 7, 8, 9 and 10, but not on profile 6. This solution-widened fracture/joint is centered at station 3+75 on resistivity profiles 7, 9 and 10, but widens considerably on profile 8.

Significant Interpretation 5 There is geophysical evidence to suggest that the solution-widened fracture associated (apparently) with sinkhole #3 extends beneath traverse 5, which is closest to the buried utility of interest.

Significant Interpretation 6: There is no geophysical evidence to suggest that traverses 6-10 are underlain by substantive voids.

SUMMARY

Analyses of the acquired geophysical data supports the conclusion that sinkholes #1 and #3 developed along or adjacent to N/S-trending solution-widened joints/fractures. [It is certainly possible that E/W-trending joints/fractures are also present in the study area. However these features (if present) cannot be confidently identified on the resistivity profiles because of their orientation.] The N/S-trending solution-widened fracture associated with sinkhole #1 does not appear to extend beneath traverses 1 and 2, which are closest to the buried utility of interest. Similarly, the solution-widened fracture associated with sinkhole #3 does not appear to extend beneath traverses 6, which is closest to the buried utility.

There is no indication that any of the geophysical traverses, with the possible exception of traverse 5, overlies air-filled voids of any significant size. As noted in the discussion of sinkhole #1, four shallow zones of anomalously high resistivity are imaged along traverse 5. These anomalies could be caused by shallow, air-filled voids. However, they are more probably attributable to the presence of effectively impervious intact cap rock in the shallow subsurface.

REFERENCES

Anderson, N., Apel, D., Dezelic, V., Ismail, A. and Kovin, **O., 2006, Assessment of Karst Activity at Highway Construction Sites in Greene and Jefferson Counties, Missouri, using the Electrical Resistivity Method, proceedings of the Highway Geophysics – NDE conference, St. Louis, MO.**

FHWA, 2004, Application of Geophysical Methods to Highway Related Problems, FHWA-sponsored website: www.cflhd.gov/agm/index.htm.

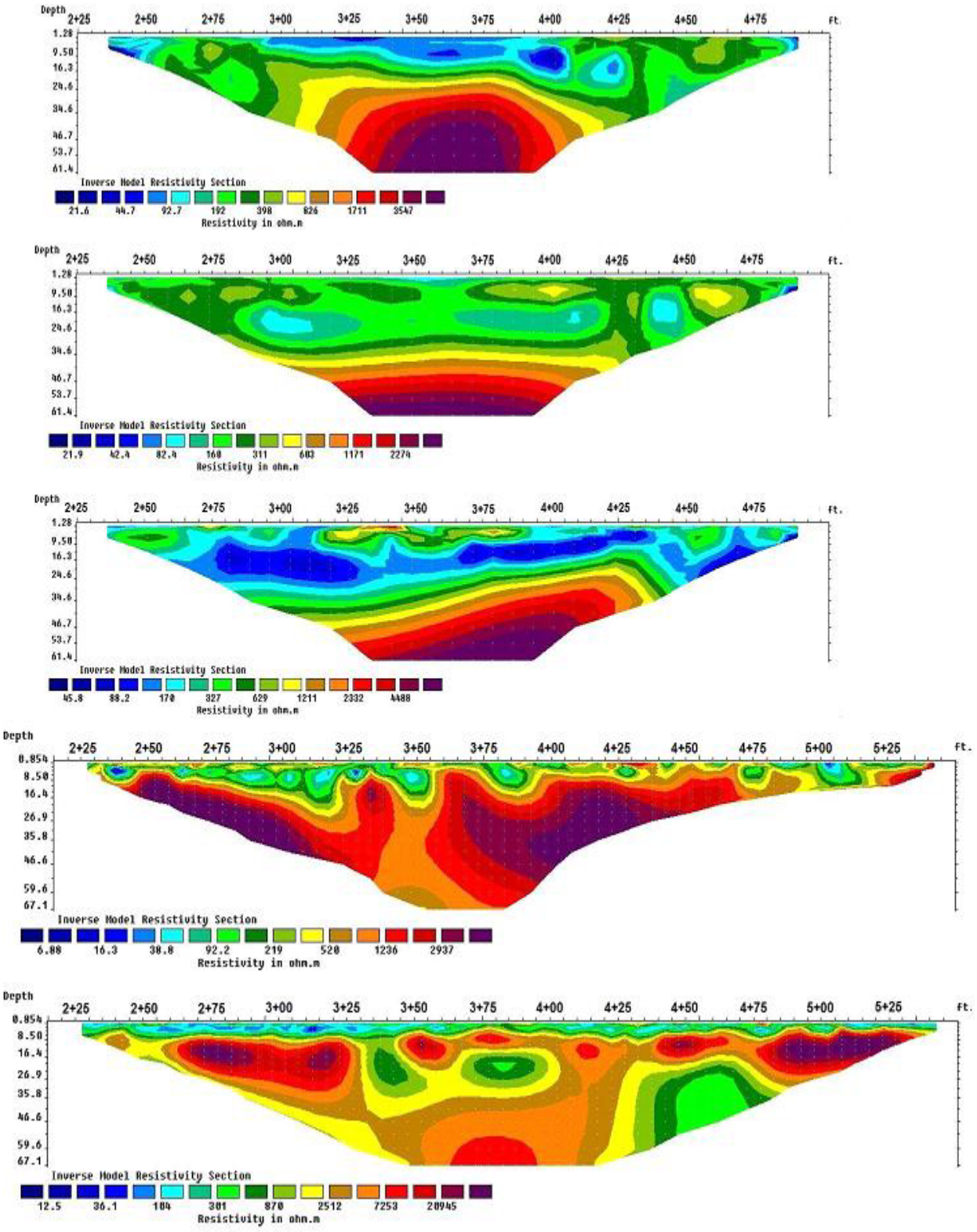

Figure 4: Electrical resistivity profiles 1-5 (top to bottom). Traverse locations are shown in Figure 1.

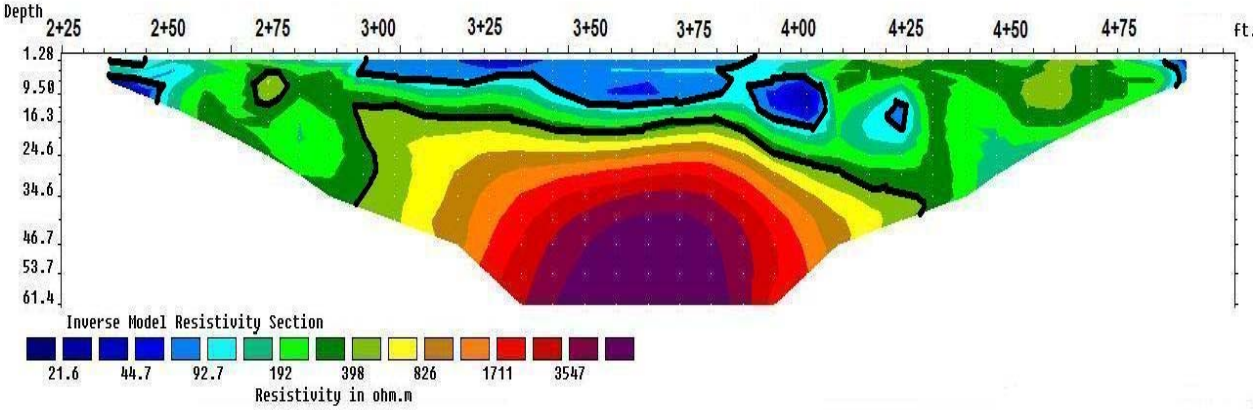

Figure 5: Interpreted electrical resistivity profile 1 (Figure 1).

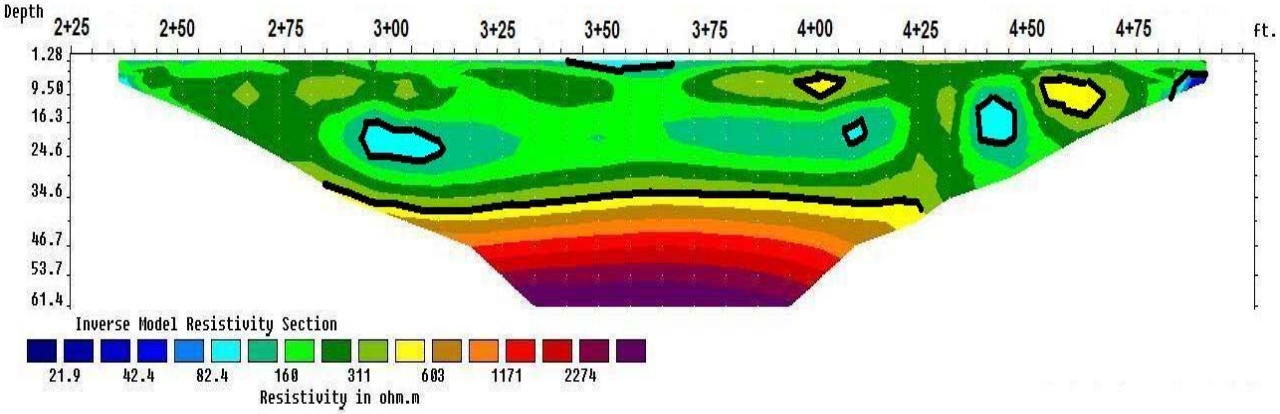

Figure 6: Interpreted electrical resistivity profile 2 (Figure 1).

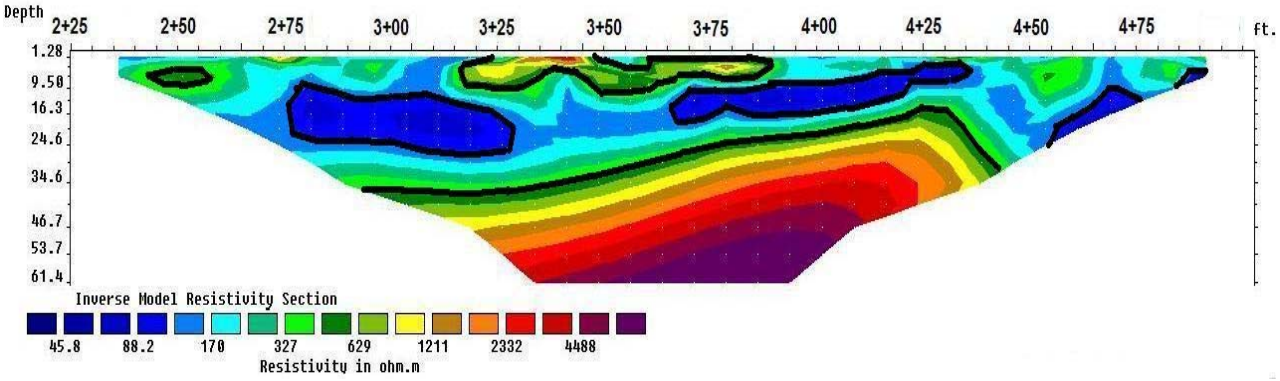

Figure 7: Interpreted electrical resistivity profile 3 (Figure 1).

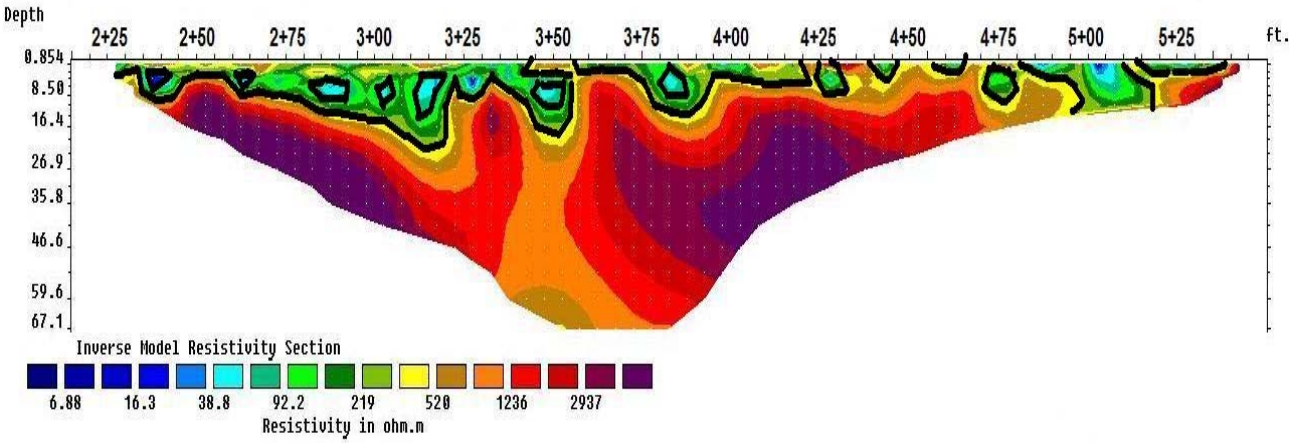

Figure 8: Interpreted electrical resistivity profile 4 (Figure 1).

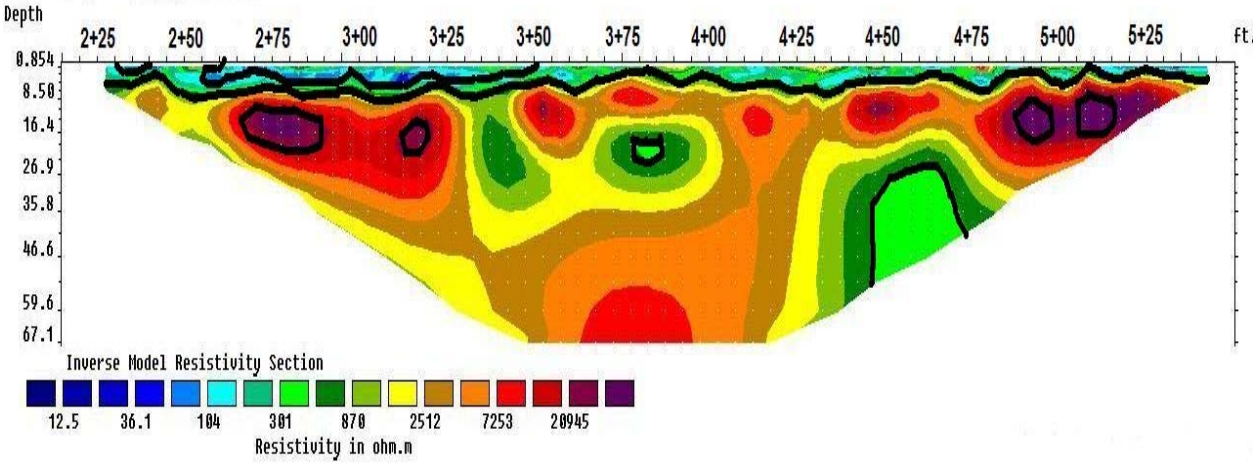

Figure 9: Interpreted electrical resistivity profile 5 (Figure 1).

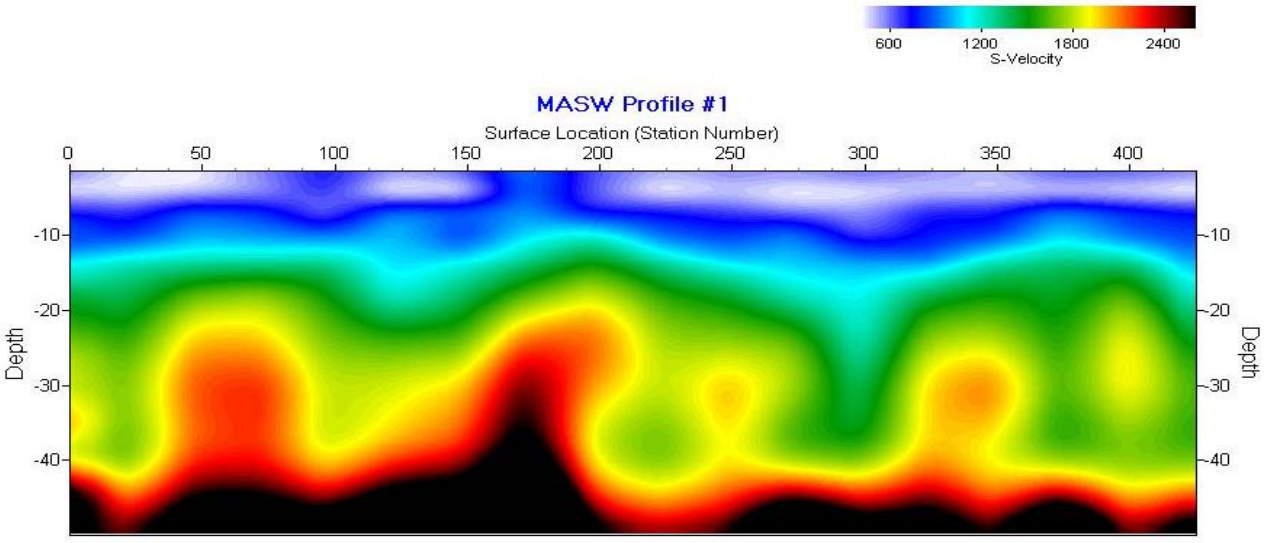

Figure 10: MASW profile 1 (Figure 1).

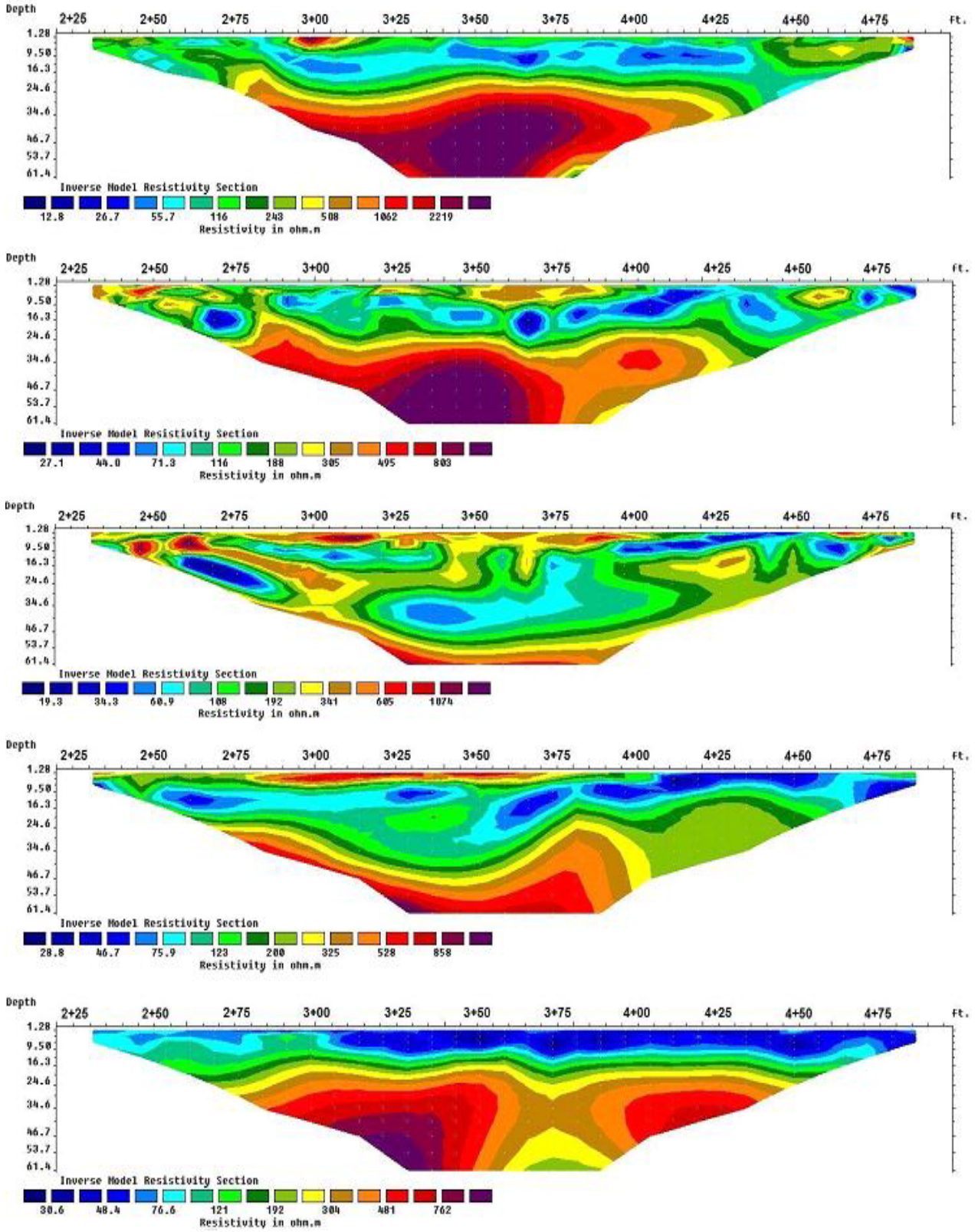

Figure 11: Electrical resistivity profiles 6-10 (top to bottom). Traverse locations are shown in Figure 1.

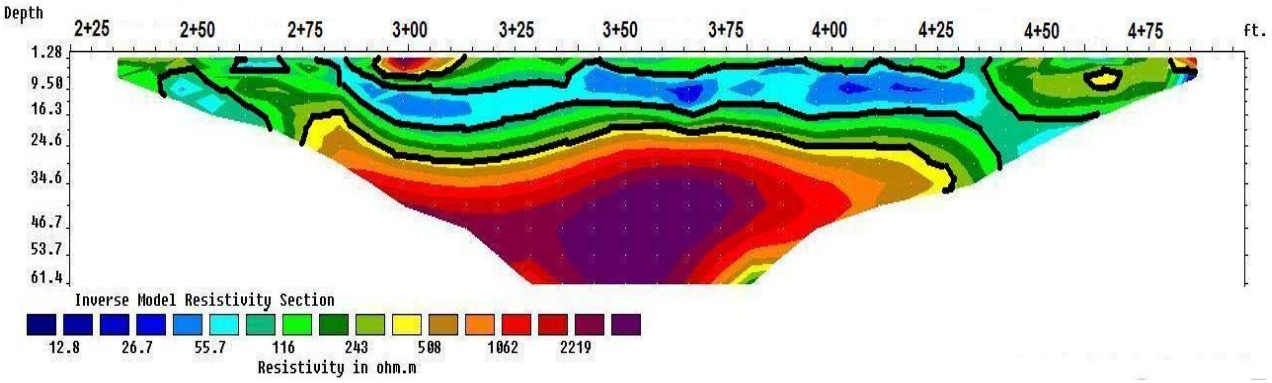

Figure 12: Interpreted electrical resistivity profile 6 (Figure 1).

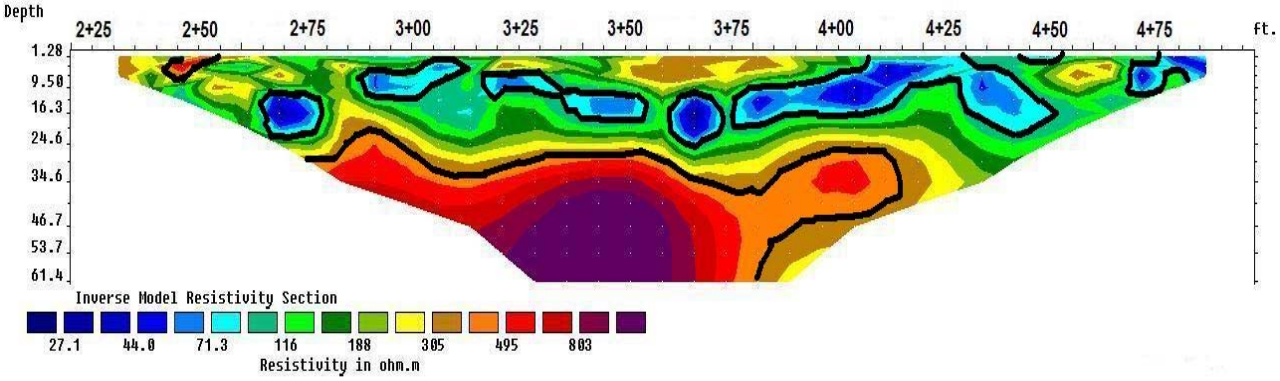

Figure 13: Interpreted electrical resistivity profile 7 (Figure 1).

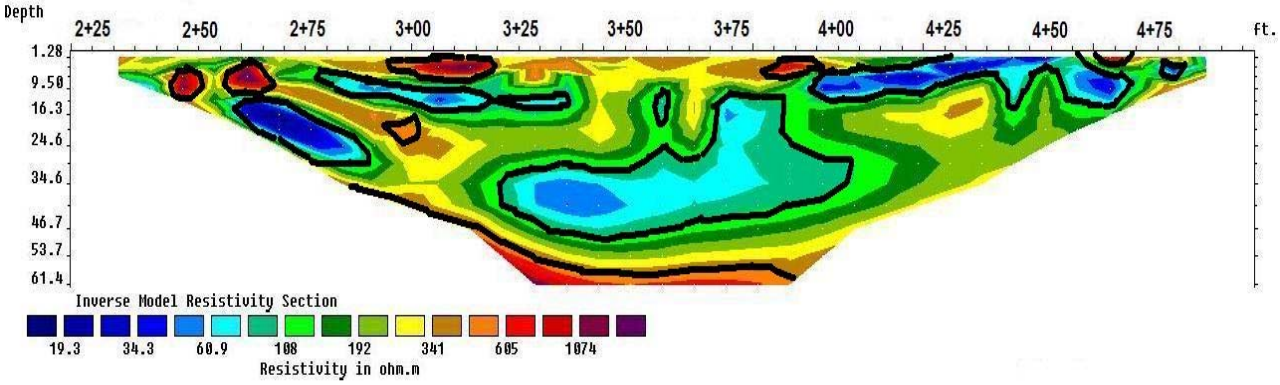

Figure 14: Interpreted electrical resistivity profile 8 (Figure 1).

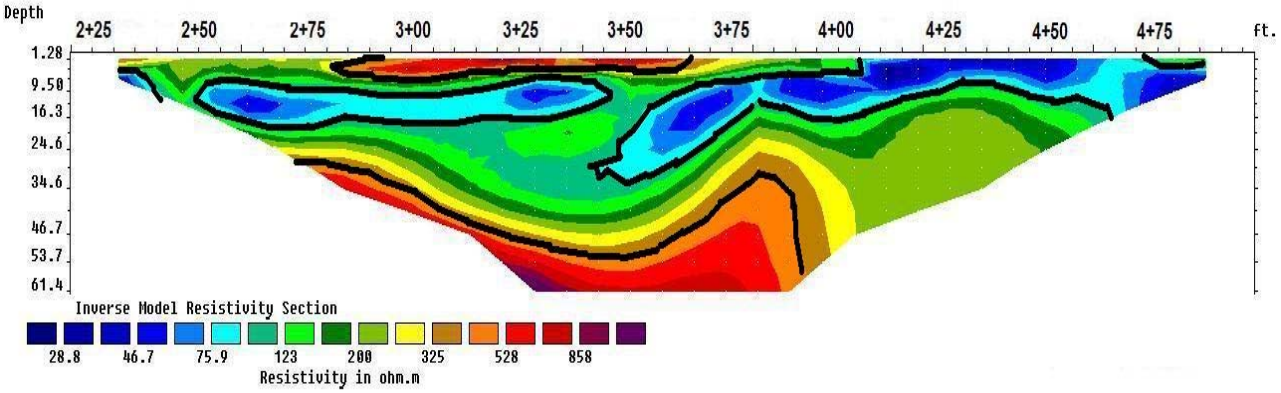

Figure 15: Interpreted electrical resistivity profile 9 (Figure 1).

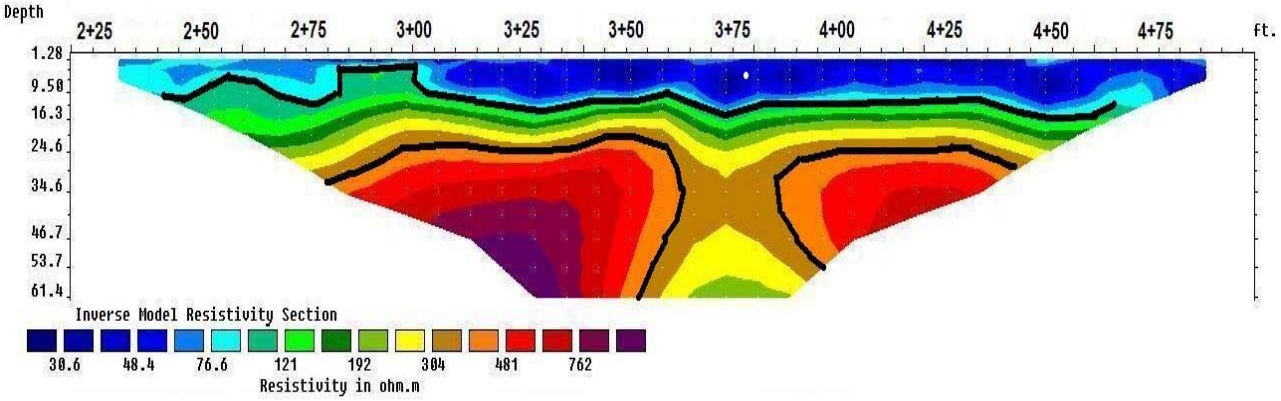

Figure 16: Interpreted electrical resistivity profile 10 (Figure 1).

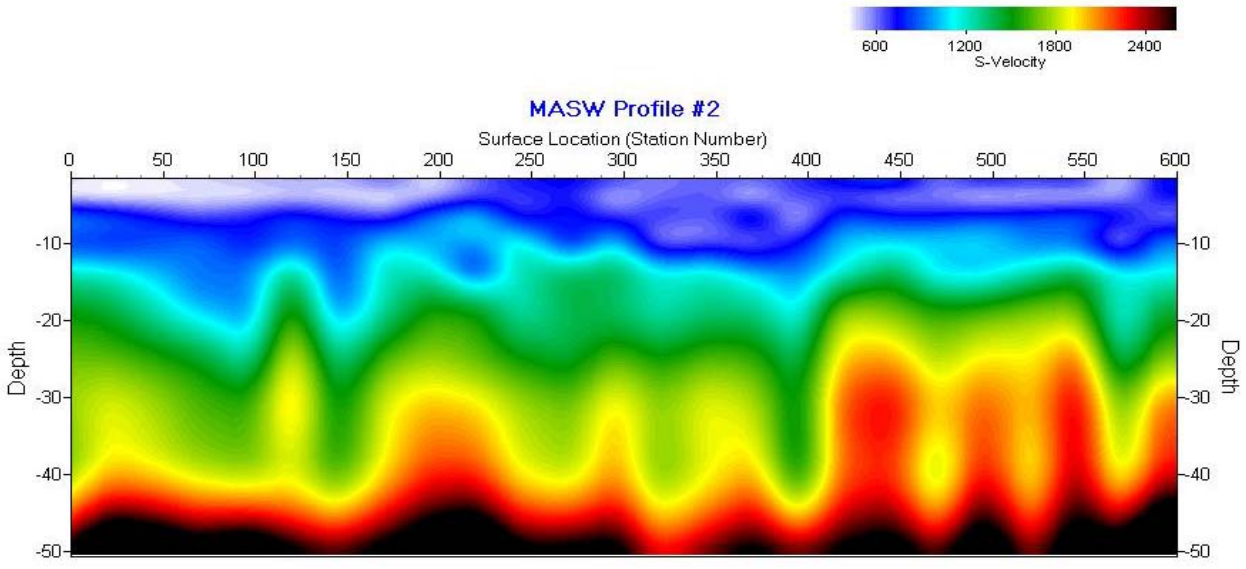

Figure 17: MASW profile 2 (Figure 1).